THERMAL-HYDRAULIC-MECHANICAL COUPLING MECHANICAL BEHAVIOR AND ACOUSTIC EMISSION CHARACTERISTICS OF DEEP SANDSTONE

by

Yi-Hang LI[a,b], He-Ping XIE[a,b,c], Ze-Tian ZHANG[b,c*], Wei-Qiang LING[c,d], Heng GAO[b], and Li REN[c,d]

[a]Guangdong Provincial Key Laboratory of Deep Earth Sciences and Geothermal Energy Exploitation and Utilization, Institute of Deep Earth Sciences and Green Energy, College of Civil and Transportation Engineering, Shenzhen University, Shenzhen, China
[b]State Key Laboratory of Hydraulics and Mountain River Engineering, College of Water Resource and Hydropower, Sichuan University, Chengdu, China
[c]MOE Key Laboratory of Deep Earth Science and Engineering, Sichuan University, Chengdu, China
[d]College of Architecture and Environment, Sichuan University, Chengdu, China

Original scientific paper
https://doi.org/10.2298/TSCI2301553L

Based on the deep in situ mining environments with "three high", a triaxial compression experiment of water-saturated sandstone under the conditions of 150 °C, 110 MPa confining stress and 105 MPa pore water stress was carried out. The results show that the creep deformation stage produces a surge in acoustic emission energy when the radial deformation of sandstone changes from expansion to rapid compression, and the sandstone is sheared by a single crack when it is damaged. From deformation monitoring and acoustic emission energy analysis, the thermal-hydraulic-mechanical (THM) coupling environment will cause irreversible changes to the internal stress distribution, pore structure and mineral framework of sandstone. In the THM coupling experiment, the irreversible impact of the rock sample due to the long-term simulation of the "three high" environment and the difference caused by the impact on the final experimental results should be considered.

Key words*: mechanical response of surrounding rock, sandstone, THM coupling, acoustic emission, triaxial compression*

Introduction

In deep geotechnical, a deep rock mass is usually subjected to thermal-hydraulic-mechanical (THM) multifield coupling [1], and high ground stress, high earth temperature, and high karst water pressure, *three high*, are the prominent environmental problems it faces [2]. In the multifield coupling environment, the mechanical response of rock is the key to the safety of engineering design, construction, and operation [3].

*Corresponding author, e-mail: zhangzetian@scu.edu.cn

Many scholars have carried out theoretical analysis and numerical simulation research on the rock mechanical response under THM environmental coupling [4-6]. In terms of experiments, Meng *et al*. [7] found that the macroscopic mechanical performance and the evolution of the internal microstructure of sandstone under THM coupling conditions are very different from those under pure heat treatment conditions. Yi *et al*. [8] analyzed the thermal-hydraulic-mechanical-chemical (THMC) coupling mechanism of brittle rocks and introduced the THMC coupling index to characterize the influence of the THMC coupling field on the stress field, thereby establishing the THMC coupling fracture criterion. Zhang *et al*. [9] and Pandey *et al*. [10] discussed the mechanism of thermal stress in rock fracture and deformation, established a THM damage coupling model, and compared the effects of various parameters on the hydraulic fracturing process.

In this paper, a triaxial compression creep experiment was carried out on sandstone. The creep time was set to 24 hours, the confining stress was set to 110 MPa, the pore water stress was set to 105 MPa, and the temperature was set to 150 °C. Additionally, the deformation and failure process of sandstone were monitored with acoustic emission. Therefore, the mechanical response law of water-saturated sandstone at different stages in an extreme multifield coupling environment was studied.

Testing information

Sandstone cores from Yibin, Sichuan, China, were selected to prepare several standard cylindrical specimens with a diameter of 50 mm and a height-diameter ratio of 2:1 [11]. To ensure that the internal pores are convenient for the application of pore water pressure, the sample with the largest permeability is selected as the test sample, with an initial porosity and permeability of 7.02% and 0.1073 mD, respectively. The experiment was carried out using an MTS 815 Flex Test GT test system with AE system at Sichuan University, fig. 1.

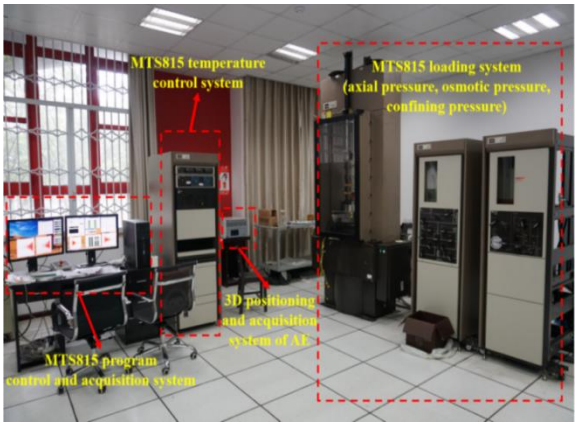

Figure 1. The MTS 815 Flex Test GT test system

When the burial depth is greater than 3500 m, the in-situ occurrence state of the deep rock mass gradually tends to the state of the hydrostatic pressure, which is a typical basic characteristic of the stress state in the deep rock mass [12]. Therefore, the designed test plan was: first, the confining stress and axial stress were increased to 3 MPa, and the pore water stress was increased to 2 MPa (to prevent high-temperature water vaporization), then, the temperature was increased to 150 °C, and then, axial and confining stresses were applied to the sample, $\sigma_1 = \sigma_3$, at a loading rate of 10 MPa per minute to 110 MPa, and finally, pore water stress was applied to the sample at a loading rate of 4 MPa per minute to 105 MPa. Considering the creep effect, when the environmental parameters are loaded to the predetermined value, the state is maintained for 24 hours, and after ensuring that the rock sample is not damaged, deviatoric stress, $\sigma_1 - \sigma_3$, is applied at 3 MPa per minute until the rock sample becomes unstable and damaged. The deformation of the sample and the acoustic emission phenomenon are monitored throughout the experiment.

Mechanical response and acoustic emission characteristics of sandstone in different stages

The temperature was 150 °C before the start of the experiment. The deformation and AE energy changes of the sandstone samples during the initial loading stage are shown in fig. 2. When the hydrostatic stress was applied, the compressive strain of the rock gradually increased in all directions, and the strain curve was concave in the time period of 0~2 minutes, indicating that some of the pores of the rock were closed under the condition of hydrostatic stress.

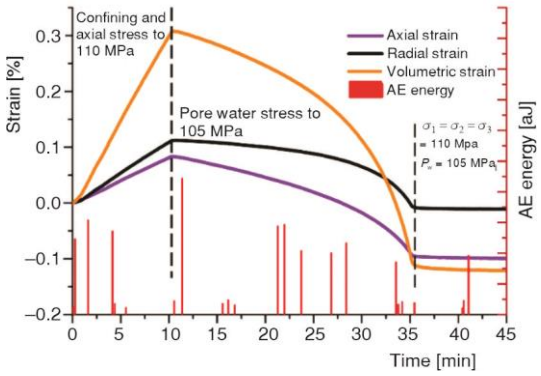

Figure 2. Deformation and acoustic emission energy variation of the sandstone sample during the loading stage

Keeping the hydrostatic stress unchanged, the strain of the specimen in each direction rapidly changed from compression to expansion when the pore water stress was applied in the axial direction. Since the pore water stress was applied by means of axial seepage, the axial strain change rate of the rock sample was more sensitive to the pore water stress. After the pore water stress was applied, pore water first entered the throats and pores that had not been closed, and as the water stress increased, pore water began to enter the cracks closed by the hydrostatic stress. Additionally, the frequency of the AE energy and the energy amplitude also increased until the pore water stress reached 105 MPa at 35 minutes and no longer continued to increase. During the loading stage, the deformation of the rock and the change in the internal microcracks were absolutely affected by the loading method.

When the environmental parameters were loaded to the predetermined values, namely, a temperature of 150 °C, hydrostatic stress of 110 MPa, and pore water stress of 105 MPa, the mechanical behavior and acoustic emission of the sandstone sample were monitored during the 24-hour period of maintaining the environment. The results are shown in fig. 3.

During the 24-hour holding period, the axial tensile strain curve gradually flattened and entered a stage similar to steady-state creep. The radial strain went through three stages before and after, and when it finally changed from expansion to compression, a large amount of AE energy was monitored.

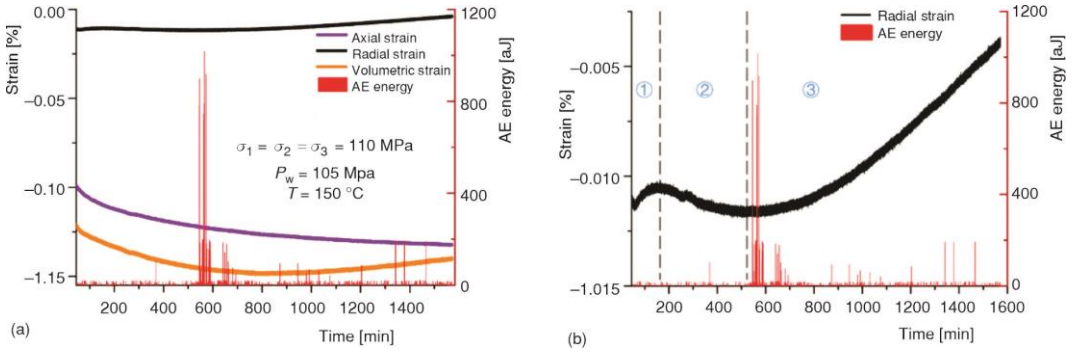

Figure 3. Deformation and acoustic emission energy variation of the sandstone sample within the 24 hours creep stage; (a) strain in all directions and (b) stages of the radial strain

At each stage, the mechanical properties of the rock are mainly limited by the development state of internal microcracks.

Stage 1: The radial direction began to transform into compression deformation. The conduction medium of confining pressure and axial pressure is the rock matrix, while the conduction of pore water pressure needs to rely on the penetration of water flow in the pores. When the pore water pressure no longer rose, due to the faster conduction of external confining pressure and axial pressure, the pores and newly generated microcracks in the rock sample affected by high-pressure pore water were recompressed.

Stage 2: In a process lasting approximately 340 minutes, due to the further conduction of pore water pressure and the increase of temperature inside the rock, the viscosity coefficient of water decreased. The flow resistance of the medium itself was reduced, the effective stress inside the rock was reduced, and the expansion of pores led to radial expansion strain. However, when the pores inside the rock sample were filled with high pressure water, most of the high pressure pore water began to enter the matrix part of the rock, and the conduction of pore water became more difficult. Additionally, the dissolution of mineral particles was strengthened by high temperature water, and the cementation strength between mineral particles was reduced. The radial strain rate decreased under 110 MPa of hydrostatic stress. Water and heat mutually enhanced each other's degradation of rock mechanical properties at the microscopic level.

Generally, sandstone is mainly composed of minerals such as quartz, feldspar, muscovite, calcite, and clay minerals. The large number of cracks inside the rock in the THM environment may be caused by the unco-ordinated deformation of minerals [13]. In addition, due to the thermal fracture of the rock sample during the heating process, the application of the load will inevitably cause initial damage to the rock sample [14]. Both will cause damage to the sandstone skeleton so that the strength of the stressed skeleton is not the same. Under the action of external hydrostatic stress, the stress will form a stress-bearing skeleton along the harder quartz and feldspar minerals, conduct concentrated transmission, and store it in the form of elastic energy on the solid skeleton **(**35-500 minutes).

Stage 3a: Due to the deterioration of rock properties by water and heat, when the skeleton of quartz or feldspar in the interior reached the threshold of skeleton damage due to stress concentration, thermal damage or the decrease in cementation strength between mineral particles, a large amount of elastic energy stored in the solid skeleton (500-700 minutes) was suddenly released, and the structure of the rock solid skeleton was adjusted. Then, the stress redistribution inside the rock in this stage caused the mineral frameworks, such as calcite and mica, whose strength and stiffness were low, to bear greater stress, so the radial strain changed from the expansion state to the compression state.

Stage 3b: On the strain-time curve, the radial compression deformation of rock rose rapidly and tended to be stable (700-1600 minutes). On the AE energy curve, due to the inability of the weak mineral framework to withstand compression, the amplitude and frequency of AE energy were significantly increased compared with before, as shown in fig. 3(b). In terms of AE spatial positioning, a concentrated acoustic emission event with relatively large energy was generated somewhere, and then the AE signal was successively emitted from all parts of the rock (presumed to be weak skeletons). Damage has already accumulated inside the sample before the formation of macroscopic cracks [15, 16], as shown in fig. 4.

The variation trends of the axial and radial directions are quite different under THM coupling conditions. Due to the mutual enhancement of high pressure pore water and heat on the degradation of the mineral skeleton at the micro level and the difference in each mineral

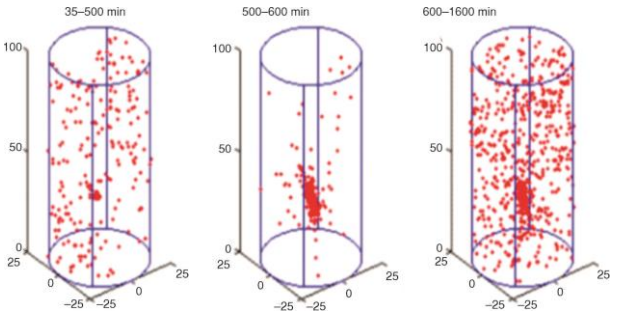

Figure 4. Acoustic emission source location of each stage in the 24 hours creep process

skeleton and the redistribution of stress, the radial deformation changed in multiple segments during the 24 hours process under the THM coupling environment, and a large amount of acoustic emission energy was produced when the final radial tension was transformed into compression.

After maintaining the extreme coupling environment for 24 hours, the rock sample was damaged by applying deviatoric stresses, $\sigma_1 - \sigma_3$, It is assumed that the overall volumetric strain of sandstone is composed of elastic volumetric strain and crack volumetric strain before entering the stage of unstable fracture propagation [17, 18]. There is the relation:

$$\varepsilon_V = \varepsilon_{eV} + \varepsilon_{cV} = \varepsilon_1 + 2\varepsilon_2 \tag{1}$$

where ε_V is the total volumetric strain, ε_{eV} – the elastic volumetric strain, ε_{cV} – the crack volumetric strain, ε_1 – the axial strain, and ε_3 – the circumferential strain. The elastic volumetric strain is given:

$$\varepsilon_{eV} = \frac{1-2\nu}{E}(\sigma_1 - \sigma_3) \tag{2}$$

where ν is the Poisson's ratio, E – the elastic modulus, σ_1 – the axial stress, and σ_3 – the confining stress. From eqs. (1) and (2), the crack volumetric strain can be written:

$$\varepsilon_{eV} = \varepsilon_1 + 2\varepsilon_3 - \frac{1-2\nu}{E}(\sigma_1 - \sigma_3) \tag{3}$$

According to eq. (3), the crack volumetric strain-axial stress curve of sandstone sample can be obtained. The mechanical parameters and characteristic stress of sandstone are shown in tab. 1.

Table 1. Physical and mechanical parameters

E [GPa] elastic modulus	ν [–] Poisson's ratio	σ_p [MPa] peak stress	σ_{cc} [MPa] crack closing stress	σ_{ci} [MPa] crack initiation stress	σ_{cd} [MPa] crack damage stress
24.30	0.22	107.50	33.48	66.79	73.64

The stress-strain curve and AE energy change during loading failure are shown in fig. 5. Since the rock sample was damaged and cracked, there was an obvious compaction Stage I. In linear elastic Stage II the stress-strain curve was roughly linear, and there was no acoustic emission energy. Stages III and IV were stable and unstable stages of crack propagation, respectively. Due to the damage caused in the previous process, the cracks penetrated to a certain extent, and the cracks could not form a stable development trend. Therefore, Stage III is very short. In Stage IV, the cracks began to penetrate further and form the failure surface, accompanied by a certain AE energy. Stage V is the postpeak stress stage. With the formation of the main failure surface, the rock began to lose stability rapidly, and the elastic energy stored in the rock began to release in large quantities, which was monitored by the AE probes.

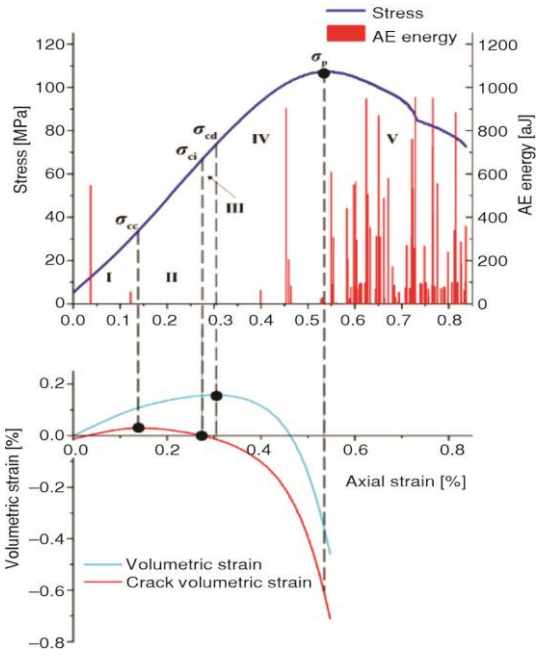

Figure 5. Stress-strain curve and AE energy variation of the failure stages

The failure mode of the sandstone sample was shear failure, which was penetrated by a single oblique shear crack, and the shear angle was approximately 33°, as shown in fig. 6. The formation of crack penetration and fracture surface of rock samples was concentrated in the postpeak stage. The stress of rock sample gradually dropped after reaching the peak strength, and there was no obvious residual stress stage. This is because the pore water pressure reduces the effective normal stress on the fracture surface and the failure surface, thereby reducing the rock strength. In the THM coupling stage, when the high-temperature and high-pressure water filled the pores and invaded the rock matrix, the mineral particles on the free surface of the rock were wetted, which weakened the connection between the particles and reduced the shear strength of the rock.

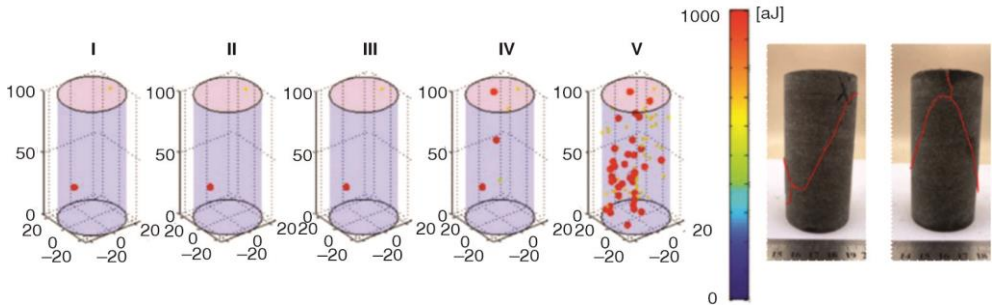

Figure 6. Acoustic emission source location and destruction form of sandstone

Furthermore, the combination of hydrophilic minerals and water in the rock further weakened the shear strength of the rock. On the other hand, as analyzed above, in the 24 hours THM coupling stage, the high temperature and high hydrostatic stress environment

caused the adjustment and destruction of the mineral skeleton structure inside the rock sample. Microcracks were initiated inside the rock sample and produced a certain degree of penetration, but the high hydrostatic pressure masked the deterioration effect. Therefore, in the failure stage, even if there is still a confining stress of 110 MPa, the rock sample will quickly fail without residual stress after reaching the peak stress, fig. 7. The long-term THM coupling environment will cause irreversible effects on the sandstone. It is further explained that under the condition of THM coupling, the difference between the physical-chemical properties of experimental rock samples when the environmental parameters just reach the preset values and after reaching the preset values for a long time needs to be considered. This difference will have a certain impact on the results of the THM experiment.

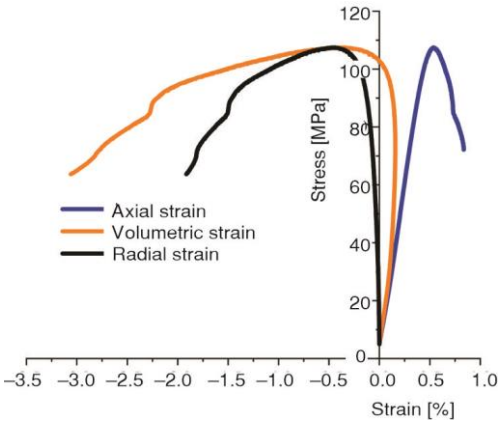

Figure 7. Stress-strain curve of the sandstone sample

Conclusion

The mechanical response and acoustic emission characteristics of sandstone under a multifield coupling environment with extremely high parameters of a 110 MPa hydrostatic stress, 105 MPa pore water stress and 150 °C were studied. When the pore water stress was applied in the axial direction, the strain rapidly changed from compression to expansion, and the final volumetric expansion strain of the rock mass reached 0.4%. During the multifield coupled creep process at high temperature and high stress, the radial deformation presented three stages of compression-expansion-rapid compression. In the process of sandstone failure, the penetration of cracks and the formation of fracture surfaces under deviatoric stress are concentrated in the postpeak stage, and there is no obvious residual stress. Therefore, a long-term THM coupling environment, which is closer to the real in situ rock state, will cause irreversible effects on the rock sample. Furthermore, the influence of irreversible deformation caused by creep should also be considered in the design, construction, and maintenance of deep engineering.

Acknowledgment

Financial supports were provided from the National Natural Science Foundation of China (Grant No. 51827901 and No. 52174084), and we are gratefully acknowledged.

Nomenclature

E – elastic modulus, [GPa]

Greek symbols

ε_V – total volumetric strain, [–]
ε_{eV} – elastic volumetric strain, [–]
ε_{cV} – crack volumetric strain, [–]
ε_1 – axial strain, [–]
ε_3 – circumferential strain, [–]
ν – poisson's ratio, [–]
σ_1 – axial stress, [MPa]
σ_3 – confining stress, [MPa]
σ_p – peak stress [MPa]
σ_{cc} – crack closing stress [MPa]
σ_{ci} – crack initiation stress [MPa]
σ_{cd} – crack damage stress [MPa]

References

[1] Tsang, C. F., *et al*., DECOVALEX Project: from 1992 to 2007, *Environmental Geology, 57* (2009), 6, pp. 1221-1237
[2] Xie, H. P., *et al*., Experimental Study on Rock Mechanical Behavior Retaining the In Situ Geological Conditions at Different Depths , *International Journal of Rock Mechanics and Mining Sciences, 138* (2021), 2, 104548
[3] Ai, T., *et al*., Changes in the Structure and Mechanical Properties of a Typical Coal Induced by Water Immersion, *International Journal of Rock Mechanics and Mining Sciences, 138* (2021), 2, 104597
[4] Li, T. J., *et al*., TOUGH-RFPA: Coupled Thermal-Hydraulic-Mechanical Rock Failure Process Analysis with Application to Deep Geothermal Wells, *International Journal of Rock Mechanics and Mining Sciences, 142* (2021), 6, 104726
[5] Rutqvist, J., *et al*., Coupled Thermal-Hydrological-Mechanical Analyses of the Yucca Mountain Drift Scale Test-Comparison of Field Measurements to Predictions of Four Different Numerical Models, *International Journal of Rock Mechanics and Mining Sciences, 42* (2005), 5, pp. 680-697
[6] Salimzadeh, S., *et al*., A Three-Dimensional Coupled Thermo-Hydro-Mechanical Model For Deformable Fractured Geothermal Systems ,*Geothermics, 71* (2018), 1, pp. 212-224
[7] Meng, T., *et al*., Evolution of Permeability and Microscopic Pore Structure of Sandstone and Its Weakening Mechanism Under Coupled Thermo-Hydro-Mechanical Environment Subjected to Real-Time High Temperature, *Engineering Geology, 280* (2021), 1, 105955
[8] Yi, W., *et al*., Thermo-Hydro-Mechanical-Chemical (THMC) Coupling Fracture Criterion of Brittle Rock, *Transactions of Nonferrous Metals Society of China, 31* (2021), 9, pp. 2823-2835
[9] Zhang, W., *et al*., Research of Fracture Initiation and Propagation in HDR Fracturing Under Thermal Stress from Meso-Damage Perspective, *Energy, 178* (2019), 7, pp. 508-521
[10] Pandey, S. N., *et al*., A Coupled Thermo-Hydro-Mechanical Modeling of Fracture Aperture Alteration and Reservoir Deformation During Heat Extraction from a Geothermal Reservoir, *Geothermics, 65* (2017), 1, pp. 17-31
[11] Ulusay, R., Hudson, J. A. *The Complete ISRM Suggested Methods for Rock Characterization, Testing and Monitoring: 1974-2006*, ISRM Turkish National Group, Ankara, 2007
[12] Xie, H. P., *et al*., Research and Development of Rock Mechanics in Deep Ground Engineering (in Chinese), *Chinese Journal of Rock Mechanics and Engineering, 34* (2015), 11, pp. 2161-2178
[13] Yang, F., *et al.* Calibrations of Thermo-Hydro-Mechanical Coupling Parameters for Heating and Water-Cooling Treated Granite, *Renewable Energy, 168* (2021), 5, pp. 544-558
[14] Wang, X. Z., *et al.*, Mechanical Properties and Acoustic Emission Characteristics of Granite Under Thermo-Hydro-Mechanical Coupling, *Thermal Science, 25* (2021), 6B, pp. 4585-4596
[15] Zha, E. S., *et al*., Long-Term Mechanical and Acoustic Emission Characteristics of Creep in Deeply Buried Jinping Marble Considering Excavation Disturbance, *International Journal of Rock Mechanics and Mining Sciences, 139* (2021), 2, 104603
[16] Jia, Z. Q., *et al*., Acoustic Emission Characteristics and Damage Evolution of Coal at Different Depths Under Triaxial Compression, *Rock Mechanics and Rock Engineering, 53* (2020), 5, pp. 2063-2076
[17] Martin, C. D., *et al*., The Progressive Fracture of Lac Du Bonnet Granite, *International Journal of Rock Mechanics and Mining Sciences & Geomechanics Abstracts, 31* (1994), 6, pp. 643-659
[18] Lu, H. J., *et al*., Mechanical Behavior Investigation of Longmaxi Shale Under High Temperature and High Confining Pressure, *Thermal Science, 23* (2019), 3A, pp. 1521-1527

Paper submitted: August 15, 2022
Paper revised: November 7, 2022
Paper accepted: November 25, 2022